Edited by Wenbin Liu Michael Ng Zhong-Ci Shi

Recent Progress in Scientific Computing

(科学计算前沿进展)

SCIENCE PRESS
Beijing

Edited by Wenbin Liu Michael Ng Zhong-Ci Shi

Recent Progress in Scientific Computing

(科学计算前沿进展)

SCIENCE PRESS
Beijing

Responsible Editor: Fan Qingkui

Published by Science Press
16 Donghuangchenggen North Street
Beijing 100717, China

Printed in Beijing

ISBN 978-7-03-019043-7 (Beijing)

Preface

There have been very rapid developments of efficient algorithms on scientific computing and related investigations of mathematical issues of partial differential equations and image processing over the past decade. As a result, many problems in diverse application fields such as fluid dynamic, image processing, computer vision, and computer graphics in the entertainment industry can now be routinely simulated to high resolution. It is our intention to organize a well respected international conference series on Scientific Computing and Partial Differential Equations in Hong Kong. The first of this conference series was held at Hong Kong Baptist University in December 2002, and was a highly successful event.

In the second of this conference series, we would like to review recent developments and to explore exciting new directions in scientific computing and partial differential equations for time dependent problems and its interaction with other fields such as image processing, computer vision and graphics. An emphasis of this conference, which we hope will set it apart from others, is the strong interaction of significant mathematics with advanced algorithms applicable to real world applications.

The Society for Industrial and Applied Mathematics (SIAM) is the major society for Applied Mathematicians. There are many chapters and sections for the SIAM in many regions in the world. The East Asia SIAM was formed a few years ago, but its first conference has not yet been held. The East Asia SIAM has recently decided to organize its first conference jointly with the 2005 International Conference on Scientific Computing and Partial Differential Equations.

The conference attracted a number of leading scientists in scientific computing and partial differential equations including

Mark Ainsworth (Strathclyde, UK),
Alfred Carasso (NIST, USA),
Carsten Carstensen (Humboldt, Germany),
Zhiming Chen (CAS, China),
Philippe G. Ciarlet (CityU, Hong Kong),
Weinan E (Princeton, USA),
Lisa Fauci (Tulane, USA),
Daniele Funaro (Modena, Italy),
Barbara Keyfitz (Fields Institute, Canada and Houston, USA),
Wenbin Liu (Kent, UK),
Yvon Maday (Paris 6, France),
Rolf Rannacher (Heidelberg, Germany),
Jie Shen (Purdue, USA),
John Strain (Berkeley, USA),
Gilbert Strang (MIT, USA),
Andrew Stuart (Warwick, UK),
Pingwen Zhang (Peking, China),
Jun Zou (CUHK, Hong Kong).

It also drew an international participants of 150. The detailed information including invited speakers, organizing committee and conference programs can be found http://www.math.hkbu.edu.hk/SCPDE05.

We are very grateful for the generous donations to support this conference given by

The Croucher Foundation,
Enrichment Programme for Young Mathematics Talents (CUHK),
Hong Kong Baptist University,
Hong Kong Mathematical Society,
K.C. Wong Education Foundation,
Lee Hysan Foundation,
PKU-HKBU Joint Research Institute for Applied Mathematics, and
Society for Industrial and Applied Mathematics.

A number of staff at Hong Kong Baptist University worked together to handle the detailed arrangements. We would especially like to thank Claudia Chui, Elsa Fong, Tammy Lam, C. W. Yeung and the graduate students of the department of Mathematics, Hong Kong Baptist University. Their help has been indispensable. We appreciate their assistance in making the conference organization a success.

These conference proceedings were refereed. We would like to thank all referees for their support. We thank Tammy Lam for the considerable work she put into producing the final layout of the proceedings.

Wenbin Liu, University of Kent, UK
Michael Ng, Hong Kong Baptist University, Hong Kong
Zhong-Ci Shi, Chinese Academy of Sciences, China
Editors
February 2007

Contents

Invited talks

Contributed Talks

Dispersive Effects of Discontinuous Galerkin FEM for Acoustics

Mark Ainsworth*

Mathematics Department, Strathclyde University, 26 Richmond Street, Glasgow G1 1XH, Scotland.

Abstract. The discontinuous Galerkin finite element method is formulated for the equations of acoustics in three dimensions based on a centred numerical flux. We show that our previous theory for the scalar advection equation may be applied in this setting and use it to show that the discrete scheme admits non-trivial propagating, Bloch-wave solutions of the homogeneous equations and bounds are given on the wave-number of the discrete waves in terms of the corresponding wave-number for plane-wave solutions of the continuous equations. Sharp bounds are established relating the order N of the scheme and the mesh-size h that are needed to provide accurate resolution of the continuous waves. As a by-product, we are able to provide a rigorous proof of the standard guideline that 'π modes per wavelength' are needed for a high order or spectral method to resolve a wave.

Key words: Discrete dispersion relation; high wave number; discontinuous Galerkin approximation; *hp*-finite element method.

AMS subject classifications: 65N50, 65N15, 65N30, 35A40, 35J05.

1. Model Problem

The equations of three-dimensional acoustics take the form

$$\begin{aligned} \rho_t + \mathbf{div}(\rho \boldsymbol{u}) &= \mathbf{0} \\ (\rho \boldsymbol{u})_t + \mathbf{div}(\rho \boldsymbol{u} \otimes \boldsymbol{u}) + \mathbf{grad} p &= \mathbf{0} \\ (p/\rho^\gamma)_t + \boldsymbol{u} \cdot \mathbf{grad}(p/\rho^\gamma) &= 0 \end{aligned} \tag{1}$$

where ρ denotes the density, p denotes the pressure and $\boldsymbol{u}$ denotes the velocity and γ is the adiabatic constant of the gas.

* Email: M.Ainsworth@strath.ac.uk

We consider a problem corresponding to an initial state where the medium is at rest and the ratio p/ρ^γ is constant everywhere. The final equation in the non-linear system then shows that the ratio remains constant in the ensuing motion, and we may therefore replace the final equation by an equation of state

$$\frac{p}{\rho^\gamma} = \text{const.} \tag{2}$$

If the ensuing disturbances are assumed to remain small, we may linearise the system about an ambient state ($\rho = \rho_0$, $p = p_0$ and $\boldsymbol{u} = \boldsymbol{0}$) and look for a solution of the form

$$\begin{aligned} \rho &= \rho_0(1 + \varepsilon\widetilde{\rho}) \\ p &= p_0(1 + \varepsilon\widetilde{p}) \\ \boldsymbol{u} &= \varepsilon\widetilde{\boldsymbol{u}} \end{aligned} \tag{3}$$

where ε is a small parameter, and $\widetilde{\rho}$, $\widetilde{p}$ and $\widetilde{\boldsymbol{u}}$ denote $\mathcal{O}(1)$ quantities. Inserting these expressions into the first two equations of (1) and equating lowest terms in ε leads to the system

$$\begin{aligned} \widetilde{\rho}_t + \mathbf{div}\widetilde{\boldsymbol{u}} &= 0 \\ \widetilde{\boldsymbol{u}}_t + (p_0/\rho_0)\mathbf{grad}\widetilde{p} &= \boldsymbol{0}, \end{aligned} \tag{4}$$

while the equation of state leads to the relation $\widetilde{p} = \gamma\widetilde{\rho}$. Hence, eliminating the pressure in favour of the density and omitting tildes, we arrive at the linearised version of (1)

$$\begin{aligned} \rho_t + \mathbf{div}\boldsymbol{u} &= 0 \\ \boldsymbol{u}_t + c^2\mathbf{grad}\rho &= \boldsymbol{0}, \end{aligned} \tag{5}$$

where $c^2 = \gamma p_0/\rho_0$ is the ambient speed of sound in the medium. Introducing the vector $\boldsymbol{U} = (\rho, \boldsymbol{u}/c)$, we may write the system in the form

$$\boldsymbol{U}_t + \boldsymbol{M}(\mathbf{grad})\boldsymbol{U} = \boldsymbol{0} \tag{6}$$

where

$$\boldsymbol{M}(\boldsymbol{w}) = \begin{bmatrix} 0 & c\boldsymbol{w}^\top \\ c\boldsymbol{w} & \boldsymbol{0} \end{bmatrix}. \tag{7}$$

Alternatively, one may eliminate the velocity to obtain a scalar wave equation for the density,

$$\rho_{tt} + c^2\Delta\rho = 0. \tag{8}$$

The nature of the physical application leads us to anticipate the presence of oscillatory wave solutions. With this in mind, we seek non-trivial solutions of the form

$$\boldsymbol{U}(\boldsymbol{x}, t) = e^{i(\boldsymbol{k}\cdot\boldsymbol{x} - \omega t)}\boldsymbol{U}_0 \tag{9}$$

where $\boldsymbol{k}$ is the *wave-vector*, ω is the temporal frequency, and $\boldsymbol{U}_0$ is a constant vector. Inserting the expressions into the linearised system and simplifying leads to the condition

$$(-\omega\boldsymbol{I} + \boldsymbol{M}(\boldsymbol{k}))\,\boldsymbol{U}_0 = \boldsymbol{0} \tag{10}$$

where $\boldsymbol{I}$ denotes the identity matrix. Hence, in order to admit a non-trivial solution, it is necessary that the matrix be singular. By considering the determinant of the matrix, we arrive at the following condition for the existence of non-trivial plane wave solutions

$$c^2\omega^2 - |\boldsymbol{k}|^2 = 0. \tag{11}$$

This relation is referred to as the *dispersion relation* for the equations. Of course, the same dispersion relation would arise if one were to insert the trial function for ρ into the scalar wave equation. The dispersion relation is important in that it relates the temporal frequency to the spatial variation in non-trivial solutions of the homogeneous equations in the absence of boundary conditions. Thus, one expects the general solution to consist of a particular solution augmented by a linear superposition of solutions of the form (9) with the wave-vector related to the frequency by the dispersion relation. For example, in the case of a time-harmonic solution, i.e. a single prescribed value of ω, corresponding to a monochromatic excitation, the magnitude of the spatial variation $|\boldsymbol{k}|$ is given by ωc with only the direction of propagation undetermined.

2. Discontinuous Galerkin Discretization

A form of the discontinuous Galerkin finite element method (DGFEM) may be traced back to [11], while overviews of more recent developments may be found in [6, 7]. The discontinuous Galerkin discretization of (5) is constructed on a partitioning of the computational domain into non-overlapping cells. Although rather general partitions may be employed for DGFEM, our chief interest here lies in investigating the ability of the numerical scheme to accurately mimic the propagation of waves through regions of free space remote from domain boundaries, where one would generally use a highly structured mesh. For this reason we shall confine our attention to uniform partitions of $\mathbb{R}^3$ consisting of cubic cells of side $h > 0$, whose sides are aligned with the coordinate axes and whose nodes are located at the points $h\mathbb{Z}^3$.

As we observed earlier, it is possible to reduce the first order system (5) to a second order scalar equation (8). However, for the purposes of discretization, it is actually more convenient to work with the first order system itself. Of course, one may regard any resulting scheme as a discretization scheme for the scalar, second-order wave equation (8) where, starting with the second-order wave equation, one rewrites the equation as a first-order system (5) before performing discretization.

For $N \in \mathbb{N}$, let $\mathbb{P}_N$ denote the usual space of polynomials in one variable of degree at most N. An N-th order DGFEM seeks an approximate solution $\boldsymbol{U}^{\mathrm{DG}}$ whose restriction to each cell K belongs to the tensor product space $\mathbb{P}_N^3(K)$, but does not require the approximation to be continuous at cell interfaces. Instead, continuity is enforced in a weak sense between neighbouring cells K and K' through the use of a numerical flux function $\widetilde{\sigma}_\gamma$ defined on the interface $\partial K \cap \partial K'$. The true flux on the interface in the direction of the unit normal $\boldsymbol{\nu}_K$ on the interface is given by

$$\boldsymbol{\sigma}(\boldsymbol{\nu}_K, \boldsymbol{U}) = \boldsymbol{M}(\boldsymbol{\nu}_K)\boldsymbol{U}.$$

The numerical flux $\widetilde{\boldsymbol{\sigma}}(\boldsymbol{\nu}_K, \boldsymbol{U}^{\mathsf{DG}})$ from cell K to cell K' in the direction of the unit outward normal $\boldsymbol{\nu}_K$ is defined by the centred scheme

$$\widetilde{\sigma}(\boldsymbol{\nu}_K, \boldsymbol{U}^{\mathsf{DG}}) = \frac{1}{2}\boldsymbol{M}(\boldsymbol{\nu}_K)(\boldsymbol{U}_K^{\mathsf{DG}} + \boldsymbol{U}_{K'}^{\mathsf{DG}}) \quad \text{on } \partial K \cap \partial K',$$

where $\boldsymbol{U}_K^{\mathsf{DG}}$ denotes the discontinuous Galerkin approximation evaluated on cell K. Observe that the flux function satisfies the consistency property $\widetilde{\boldsymbol{\sigma}}(\boldsymbol{\nu}_K, \boldsymbol{U}) = \sigma(\boldsymbol{\nu}_K, \boldsymbol{U})$ when $\boldsymbol{U}$ is continuous at an interface. Moreover, there is no generation or loss of flux in the sense that the flux from cell K to K' is exactly balanced by the flux in the opposite direction from K' to K:

$$\widetilde{\boldsymbol{\sigma}}(\boldsymbol{\nu}_K, \boldsymbol{U}^{\mathsf{DG}}) = -\widetilde{\boldsymbol{\sigma}}(\boldsymbol{\nu}_{K'}, \boldsymbol{U}^{\mathsf{DG}}) \quad \text{on } \partial K \cap \partial K'$$

where $\boldsymbol{\nu}_{K'}$ denotes the outward normal on $\partial K'$. More general numerical fluxes and the associated dispersive and dissipative properties of the resulting schemes were discussed in [3].

Multiplying the equation (6) by a test function $\boldsymbol{V}$, and applying integration by parts results in the following equation,

$$(\boldsymbol{U}_t, \boldsymbol{V})_K = (\boldsymbol{U}, \boldsymbol{M}(\mathbf{grad})\boldsymbol{V})_K - \int_{\partial K} \boldsymbol{V}^\top \boldsymbol{\sigma}(\boldsymbol{\nu}_K, \boldsymbol{U})\, \mathrm{d}s \tag{12}$$

where the final term represents the transfer of flux across the cell face. This equation is satisfied by the true solution of the system (6). The *discontinuous Galerkin finite element approximation* of the problem is defined by replacing the true solution in the first two terms by its approximation $\boldsymbol{U}_K^{\mathsf{DG}} \in \mathbb{P}_N^3(K)$ on cell K, and replacing the true flux $\boldsymbol{\sigma}(\boldsymbol{\nu}_K, \boldsymbol{U})$ with the centred numerical flux $\widetilde{\boldsymbol{\sigma}}(\boldsymbol{\nu}_K, \boldsymbol{U}^{\mathsf{DG}})$ and requiring that

$$(\boldsymbol{U}_{K,t}^{\mathsf{DG}}, \boldsymbol{V})_K = (\boldsymbol{U}_K^{\mathsf{DG}}, \boldsymbol{M}(\mathbf{grad})\boldsymbol{V})_K - \int_{\partial K} \boldsymbol{V}^\top \widetilde{\boldsymbol{\sigma}}(\boldsymbol{\nu}_K, \boldsymbol{U}^{\mathsf{DG}})\, \mathrm{d}s \tag{13}$$

holds for all test functions $\boldsymbol{V} \in \mathbb{P}_N^3(K)$. This defines the scheme, which takes the form of a coupled system of first order ordinary differential equations in time along with an initial condition in terms of the initial state of the system. A fully discrete scheme would entail discretization of the temporal derivative, but we shall content ourselves with a study of the spatial discretization and not pursue this further here [8].

3. Existence of Bloch Waves for DGFEM

We have seen that the true equation admits non-trivial propagation plane waves of the form

$$\boldsymbol{U}(\boldsymbol{x}, t) = e^{-i\omega t} e^{i\boldsymbol{k}\cdot\boldsymbol{x}} \boldsymbol{U}_0$$

provided that the wave-vector $\boldsymbol{k}$ is related to the frequency ω by the dispersion relation (11). One might wonder whether the numerical scheme admits non-trivial propagating discrete solutions, and if so, how the wave-number for the discrete solutions was related to that of the continuous solutions. Obviously, the discontinuous

Galerkin approximation space does not contain plane wave solutions, so we should first settle on the form and the properties that the propagating discrete solutions should have.

By analogy with the plane wave used in the continuous setting, we seek non-trivial solutions of the form

$$\boldsymbol{U}^{\mathsf{DG}}(\boldsymbol{x},t) = e^{-i\omega t}\varepsilon(\boldsymbol{x})\boldsymbol{U}_0 \tag{14}$$

where $\varepsilon \in \mathbb{P}_N^3(K)$ on each cell K. Naturally, we require that this function should satisfy the discretization scheme (13). In fact, it will be convenient to rewrite the scheme by integrating by parts, to obtain the equivalent condition

$$(\boldsymbol{U}_{K,t}^{\mathsf{DG}} + \boldsymbol{M}(\mathbf{grad})\boldsymbol{U}_K^{\mathsf{DG}}, \boldsymbol{V})_K + \frac{1}{2}\int_{\partial K} \boldsymbol{V}^\top \boldsymbol{M}(\boldsymbol{\nu}_K)(\boldsymbol{U}_{K'}^{\mathsf{DG}} - \boldsymbol{U}_K^{\mathsf{DG}})\,\mathrm{d}s = 0. \tag{15}$$

Finally, the plane waves have the following *Bloch wave* [10] property:

$$\boldsymbol{U}(\boldsymbol{x} + h\boldsymbol{m}, t+\tau) = e^{i(h\boldsymbol{k}\cdot\boldsymbol{m} - \omega\tau)}\boldsymbol{U}(\boldsymbol{x},t) \quad \forall \boldsymbol{m} \in \mathbb{Z}^3, \forall \tau \in \mathbb{R}.$$

That is to say, translation of the solution in space or shift in time is equivalent to a change of phase. By the same token, we ask that the discrete solution should have the same property

$$\boldsymbol{U}^{\mathsf{DG}}(\boldsymbol{x} + h\boldsymbol{m}, t+\tau) = e^{i(h\widetilde{\boldsymbol{k}}\cdot\boldsymbol{m} - \omega\tau)}\boldsymbol{U}^{\mathsf{DG}}(\boldsymbol{x},t) \quad \forall \boldsymbol{m} \in \mathbb{Z}^3, \forall \tau \in \mathbb{R}, \tag{16}$$

where $\widetilde{\boldsymbol{k}}$ is the *discrete wave-vector*.

In general, we shall see that $\widetilde{\boldsymbol{k}}$ differs from $\boldsymbol{k}$, reflecting the fact the discrete scheme does not admit waves that propagate at precisely the same speed as for the continuous equation. Thus, the numerical waves might possibly lead or lag behind the continuous wave depending on the particular excitation ω and, in the case of a superposition, one might see *dispersive* effects in the numerical scheme that are not present in the continuous equations. Moreover, we may find that $\widetilde{\boldsymbol{k}}$ contains non-zero imaginary part, corresponding to numerical *attenuation* or *dissipation*. For further discussion on the dispersion and dissipation of numerical schemes, we refer to [9, 13].

We wish to show that there exist non-trivial functions $\boldsymbol{U}^{\mathsf{DG}}$ of the form (14), satisfying conditions (15) and (16). Furthermore, in order to understand the nature of the numerical scheme, we wish to relate the components of the discrete wave-vector $\widetilde{\boldsymbol{k}}$ to those of the corresponding continuous wave-vector $\boldsymbol{k}$.

Our main result may be stated formally as follows:

Theorem 1. *Suppose that $\omega \in \mathbb{R}$ and wave-vector $\boldsymbol{k} \in \mathbb{R}^3$ satisfy the continuous dispersion relation $|\boldsymbol{k}|^2 = \omega^2 c^2$. Then, there exists a corresponding discrete wave-vector $\widetilde{\boldsymbol{k}} \in \mathbb{C}^3$ and a non-trivial discrete Bloch-wave solution $\boldsymbol{U}^{\mathsf{DG}}$ of the form* (14) *satisfying conditions* (15) *and* (16).

To see why the result is true, we fix any particular cell $K = \prod_{\ell=1}^3 (a_\ell, b_\ell)$, with $b_\ell - a_\ell = h$. In [2, Section 5], we showed there exists $\varepsilon_\ell \in \mathbb{P}_N(a_\ell, b_\ell)$ satisfying the condition

$$ik_\ell(\varepsilon_\ell, v) = (\varepsilon_\ell', v) + \frac{1}{2}\left(\lambda_\ell \varepsilon_\ell(a_\ell) - \varepsilon_\ell(b_\ell)\right) v(b_\ell) + \frac{1}{2}\left(\varepsilon_\ell(a_\ell) - \lambda_\ell^{-1}\varepsilon_\ell(b_\ell)\right) v(a_\ell) \tag{17}$$

for all $v \in \mathbb{P}_N(a_\ell, b_\ell)$, where $\lambda_\ell = e^{ih\widetilde{k}_\ell}$ with $\widetilde{k}_\ell$ as in the statement of our theorem. We use these function to construct the choice of ε in the expression (14) on element K by setting $\varepsilon(\boldsymbol{x}) = \prod_{\ell=1}^{3} \varepsilon_\ell(x_\ell)$. The value of $\boldsymbol{U}^{\mathsf{DG}}$ on the remaining cells is then *defined by* the condition (16). That is to say, we evaluate $\boldsymbol{U}^{\mathsf{DG}}$ at a given point in a cell by first evaluating $\boldsymbol{U}^{\mathsf{DG}}$ at the corresponding point in cell K, and then multiplying by the phase indicated in (16).

It remains only to show that the function $\boldsymbol{U}^{\mathsf{DG}}$ satisfies (15) on the particular cell K, since the result in case of the remaining cells would then follow automatically thanks to condition (16). Inserting the expression (14) into (15) and simplifying leads to the following condition on $\boldsymbol{U}_0$:

$$\mathbf{0} = -i\omega \boldsymbol{U}_0 + \sum_{\ell=1}^{3} \frac{Q_\ell(v)}{(\varepsilon_\ell, v)} \boldsymbol{M}(\boldsymbol{e}_\ell)\boldsymbol{U}_0, \quad \forall v \in \mathbb{P}_N(a_\ell, b_\ell),$$

where $\boldsymbol{e}_\ell$ denotes the ℓ-th unit cartesian vector, and

$$Q_\ell(v) = (\varepsilon_\ell, v) + \frac{1}{2}\left(\varepsilon_\ell(b_\ell^+) - \varepsilon_\ell(b_\ell^-)\right) v(b_\ell) + \frac{1}{2}\left(\varepsilon_\ell(a_\ell^+) - \varepsilon_\ell(a_\ell^-)\right) v(a_\ell).$$

We may simplify $Q_\ell(v)$ by taking advantage of condition (16) to write $\varepsilon_\ell(b_\ell^+) = \lambda_\ell \varepsilon_\ell(a_\ell^+)$ and $\varepsilon_\ell(a_\ell^-) = \lambda_\ell^{-1}\varepsilon_\ell(b_\ell^-)$. Inserting these into the expression for Q_ℓ and using equation (17), we see that

$$Q_\ell(v) = ik_\ell(\varepsilon_\ell, v).$$

The condition on $\boldsymbol{U}_0$ then simplifies to read

$$\mathbf{0} = -i\left(\omega \boldsymbol{I} - \boldsymbol{M}(\boldsymbol{k})\right)\boldsymbol{U}_0,$$

and, in view of our assumption on ω and $\boldsymbol{k}$, on recalling (10) we see that non-trivial solutions exist as claimed.

Theorem 1 shows that the numerical scheme mimics the continuous system in the sense that if the continuous system admits a propagating wave with wave-vector $\boldsymbol{k}$, then the numerical scheme also admits a corresponding wave with wave-vector $\widetilde{\boldsymbol{k}}$. The next result quantifies in what sense $\widetilde{\boldsymbol{k}}$ may be regarded as an approximation to $\boldsymbol{k}$.

Theorem 2. *Let $\boldsymbol{k}$ and $\widetilde{\boldsymbol{k}}$ be defined as in Theorem 1. Then*

$$e^{ih(\widetilde{k}_\ell - k_\ell)} = 1 + q_N + \mathcal{O}(|q_N|^2) \tag{18}$$

where

$$q_N = \frac{H_N(-ihk_\ell)e^{ihk_\ell}\mathcal{E}_N + (-1)^{N+1}H_N^*(-ihk_\ell)e^{-ihk_\ell}\mathcal{E}_N^*}{H_N(-ihk_\ell)e^{ihk_\ell} + (-1)^N H_N^*(-ihk_\ell)e^{-ihk_\ell}} \tag{19}$$

and $H_N(\cdot)$ denotes the confluent hypergeometric function ${}_1\mathrm{F}_1(-N; -2N-1; \cdot)$, $\mathcal{E}_N$ is the relative error in the $[N+1/N]$-Padé approximate to e^{ihk_ℓ}, and * denotes complex conjugation.

A proof of this result will be found in [2].

3.1 Behaviour in the limit $hk \ll 1$

The order in hk for the difference between the discrete wave-number and the true wave-number is often used as a criterion for comparing, and even the design [5] of, numerical schemes for wave propagation. Suppose that $hk_\ell \ll 1$, then we find [2] to leading order in hk that

$$e^{ih(\widetilde{k}_\ell - k_\ell)} = 1 + \frac{i}{2}\left[\frac{N!}{(2N+1)!}\right]^2 \begin{cases} -(hk_\ell)^{2N+3}\dfrac{N+1}{2N+3}, & N \text{ even} \\ (hk_\ell)^{2N+1}\dfrac{2N+1}{N+1}, & N \text{ odd} \end{cases} \tag{20}$$

and as a consequence, again to leading order in hk,

$$\widetilde{k}_\ell - k_\ell = \frac{1}{2}\left[\frac{N!}{(2N+1)!}\right]^2 \begin{cases} -h^{2N+2}k_\ell^{2N+3}\dfrac{N+1}{2N+3}, & N \text{ even} \\ h^{2N}k_\ell^{2N+1}\dfrac{2N+1}{N+1}, & N \text{ odd.} \end{cases} \tag{21}$$

Figure 1 shows the variation of the actual relative errors $(h\widetilde{k} - hk)/hk$ versus hk for the discontinuous Galerkin approximations of orders 1 through 5. It is seen that the the above asymptotic orders are realised provided that hk is sufficiently small. However, we see that when hk is not sufficiently small, then the relative error is of order 1 and behaves rather erratically. This phenomenon is familiar to members of the computational wave propagation community, where one often hears the rule of thumb recommending that *ten elements per wavelength* should be used to resolved a wave using first order elements. In the present context, we see that the wavelength $\lambda = 2\pi/k$ so that the number of elements per wavelength is roughly $2\pi/hk$. The rule of thumb would suggest using $hk < \pi/5 \approx 0.6$ in practical computations, and examining Figure 1 one sees that this indeed provides good resolution for first order elements, but is rather conservative for the higher order elements. We shall have more to say on this topic in Section 4.2.

As alluded to earlier, we may regard the discontinuous Galerkin approximation of the first-order system (5) as a non-standard approximation scheme for the second-order scalar wave-equation (8). It therefore makes sense to compare these results with those conjectured by Thompson and Pinsky [12], and subsequently proved in [1, 4], for standard conforming Galerkin finite element approximation of the second order wave equation:

$$\widetilde{k}_{CG} - k = \mathcal{O}(h^{2N}k^{2N+1})$$

We see that in the limit $hk_\ell \ll 1$, the phase accuracy of the discontinuous Galerkin method and the conforming Galerkin method is comparable in the case of elements of *odd* order. However, discontinuous Galerkin using *even* order elements is superior to the continuous Galerkin formulation by two orders of hk, and is actually just as good as that of the element of next highest order. This suggests that the use of even order elements in conjunction with discontinuous Galerkin approximation with

centred fluxes as an approximation scheme for the second-order scalar wave equation has potential advantages over standard Galerkin schemes in terms of phase accuracy.

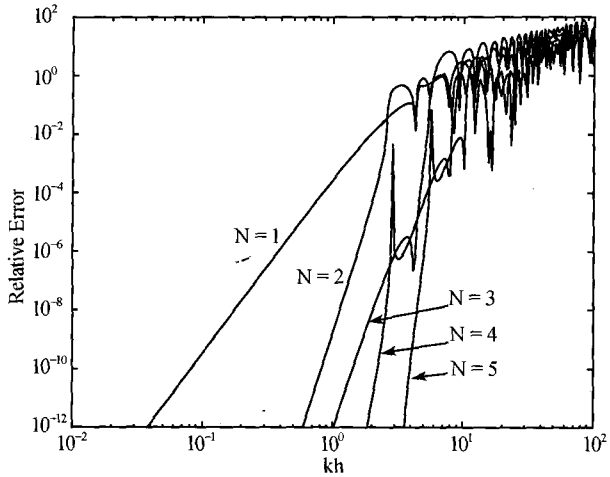

Figure 1 Relative error in the approximation of $\widetilde{k}$ of wave-number k as hk varies along with theoretical asymptotic rates of decay given in (21) shown as straight lines.

3.2 Behaviour for large order N and large wave-number hk

Examining the estimates (21) further, one is struck by the rapid decay of the multiplicative constant in the leading term in the error as the order N is increased. This suggests, but of course does not prove, that fixing the mesh-size h and increasing the order N of the method might offer some advantages compared with the traditional approach whereby the order N is fixed, and the mesh-size reduced.

In Figure 2, we show the real and imaginary parts of the relative error in the approximation of the wave-number on a fixed mesh-size for various values of hk, as the order N of the method is increased. A quick comparison with the corresponding Figure 1 for low order methods shows the same basic features whereby the error makes a transition from an oscillatory phase to a monotonically decreasing phase once the number of degrees of freedom (here related to the order N) is sufficiently large compared with hk. However, a closer examination reveals some significant differences. Firstly, the number of degrees of freedom is shown on a linear scale in Figure 2 as opposed to a logarithmic scale in Figure 1. Thus, the reduction in the error in the asymptotic case is now at least *exponential* in terms of the number of degrees of freedom as opposed to *algebraic* in the case of the low order methods. Secondly, the change from oscillatory behaviour to monotonic decay is increasingly marked as hk is increased with the *threshold* is located at $N \approx hk/2$.

The following result [2] on the behaviour of q_N appearing in Theorem 2 confirms that these simple observation are true in general:

Theorem 3. *Let q_N denote the quotient appearing in the expression for the error in Theorem 1. Then,*

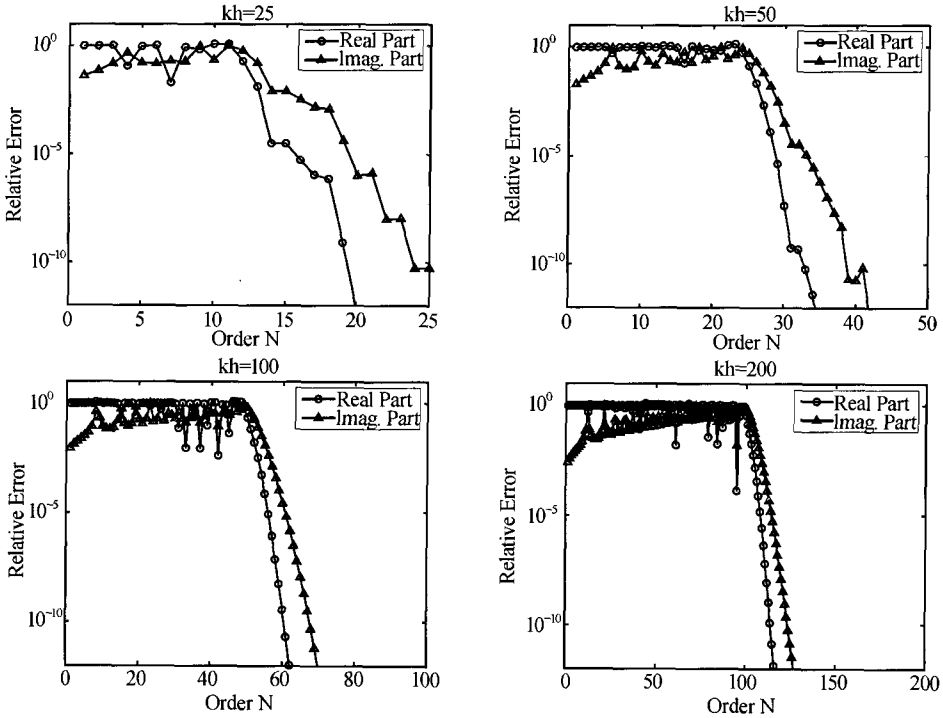

Figure 2 Real and imaginary parts of relative error q_N for the approximation of the physical mode e^{ihk} for hk=25, 50, 100, 200.

- *if* $2N+1 < hk - C(hk)^{1/3}$, *then* q_N *oscillates but does not decay as* N *is increased;*
- *if* $hk - o(hk)^{1/3} < 2N+1 < hk + o(hk)^{1/3}$, *then* q_N *decays algebraically at a rate* $\mathcal{O}(N^{-1/3})$.
- *if* $2N+1 \gg hk$, *then* q_N *decays at a super-exponential rate as* $N \to \infty$,

$$q_N \approx -\left(\Upsilon_N(hk) - \frac{ihk}{2N+3}\right)\left[\frac{ehk}{2\sqrt{(2N+1)(2N+3)}}\right]^{2N+2} \tag{22}$$

where

$$\Upsilon_N(hk) = \frac{(1-\gamma)e^{i(hk+\psi_N)} + (-1)^{N+1}(1+\gamma)e^{-i(hk+\psi_N)}}{(1-\gamma)e^{i(hk+\psi_N)} + (-1)^{N}(1+\gamma)e^{-i(hk+\psi_N)}}$$

and $\psi_N = \arg {}_1\mathrm{F}_1(-N; -2N-1; -ihk)$.

Theorem 3 shows that the asymptotic rate of reduction is actually *super-exponentially fast.* Moreover, both theory and practice show that there is a *sharp transition* from an essentially unresolved state, where the relative error is of order